EVALUATION OF RANGE OF STABLE OPERATION OF HYDRAULIC TURBINE BASED ON 1D-3D MODEL OF FULL LOAD PULSATIONS

Denis CHIRKOV*

Institute of Computational Technologies SB RAS, Novosibirsk, Russia

Sergey CHERNY

Institute of Computational Technologies SB RAS, Novosibirsk, Russia

Pavel SCHERBAKOV

Novosibirsk State University, Novosibirsk, Russia

Alexander ZAKHAROV

OJSC "Power Machines" LMZ, St-Petersburg, Russia

ABSTRACT

Operation of Francis turbines at very high discharge is bounded by full load surge phenomenon, caused by instability of two-phase swirling flow downstream the runner. Recently the authors presented a hybrid 1D-3D model and numerical algorithm for simulation of this phenomenon. In present work this numerical model is further enhanced and applied to prediction of limit of stable operation of prototype hydro-power plant. First, the influence of full runner computations rather than one runner channel is investigated. Then, the frequency of pressure pulsations compared with first unstable frequency, obtained in frames of fully 1D model. It is shown that if cavitation compliance is identified from unsteady 1D-3D computation, then first unstable frequency is very close to that, obtained in 1D-3D simulation. This fact establishes the bridge between 3D CFD and fully 1D models of full load surge. A series of unsteady computations for various operating points (guide vane openings) and various Thoma numbers are carried out. Based on these results the zone of unstable operation is evaluated for two runner modifications. The onset of strong power pulsations is in good agreement with experimental data, measured at prototype, showing practical applicability of this approach.

KEYWORDS

full load, instability, self-excited pulsations, CFD simulation

1. INTRODUCTION

Wide range of stable operation is one of main targets in Francis turbine design. In partial load this range is restricted by pressure pulsations, induced by helical vortex rope, formed in the draft tube. At high load this range is restricted from cavitational considerations and risk of strong self-exited oscillations [1, 2]. The reason of these oscillations is the hydraulic instability of cavitating flow in the draft tube. The whole hydraulic system of the power plant

* *Corresponding author:* Institute of Computational Technologies SB RAS, acad. Lavrentiev avenue 6, Novosibirsk, Russia, phone: +7(383)3307373, email: chirkov@ict.nsc.ru

gives positive feedback to small perturbation of cavity volume, enforcing cavity pulsations. The problem was reported for several prototype turbines [2 - 4]. Full load surge phenomenon was also reproduced in scale model tests, see [4, 5].

Practice shows that the amplitude and frequency of self-oscillations strongly depend on the velocity profile formed downstream the runner. Thus the onset and intensity of self-oscillations is runner dependent. Therefore it is desirable to predict the upper limit of stable operation of prototype turbine at the early stage of runner design.

Physical mechanism of full-load instability is well explained using simple 1D models, using the concepts of cavitation compliance $C = -\partial V_c / \partial p$ and mass flow gain factor (MFGF) $\chi = -\partial V_c / \partial Q$ [3, 6, 7]. 1D models establish the fact of instability and determine the frequency of unstable modes, however practical application of such models for the prediction of amplitudes of pressure pulsations is problematic. In order to evaluate the amplitude of limit cycle one have to perform time domain simulation using non-linear system with operating point dependent compliance and MFGF [3]. Obtaining these dependencies requires series of two-phase CFD computations for different operating points. Moreover, as it will be shown in the present paper, steady-state CFD can be inadequate for determination of true values of C and χ.

Recently the present authors proposed a hybrid 1D-3D two-phase model of the whole hydraulic power plant, including penstock and turbine itself [8, 9]. The model combines 1D hydro-acoustic equations for the penstock and 3D unsteady Reynolds-Averaged Navier-Stokes (RANS) equations for the turbine. The model is able to capture and directly simulate self-oscillations in full load. In [9] we studied the influence of computational grid and time step size. Moreover, computed pressure pulsations were compared to experimental data, measured for n_q=48.3 turbine, operated at maximum head $H = 220$ m. The present work continues investigations, started in [9]. First, computations of old-designed runner R1 are refined by considering all runner channels rather than one (periodic) channel, used in [9]. Then the influence of operating point, namely the discharge and Thoma number, is investigated. Based on the obtained results, the limit of stable operation at high discharge is evaluated and compared to experimental data measured in prototype.

2. 1D-3D MODEL OF HYDRAULIC POWER PLANT

The 1D-3D model, developed in [8, 9], consist of 1D hydro-acoustic equations of penstock and two-phase RANS equations of cavitating flow in turbine, see Fig. 1. Hydro-acoustic equations of penstock of length L_p are

$$\begin{cases} \dfrac{\partial h}{\partial t} + \dfrac{a^2}{gA}\dfrac{\partial Q}{\partial x} = 0, \\ \dfrac{\partial Q}{\partial t} + gA\,\dfrac{\partial h}{\partial x} = 0, \end{cases} \qquad x \in [0, L_p]. \tag{1}$$

Here $h = p/(\rho_L g) - z$ is the piezometric head (note, that Oz axis is directed downwards); Q is the discharge; a is the wave speed; A is the cross section of penstock; t is time and x is the coordinate along the length of the penstock.

Cavitating flow inside the turbine is described by unsteady 3D RANS equations for isothermal compressible “liquid–vapor” mixture with mixture density

$$\rho = \alpha_L \rho_L + (1 - \alpha_L)\rho_V .$$

Spatial distribution of liquid volume fraction α_L is governed by transport equation

$$\frac{\partial \alpha_L}{\partial t} + \operatorname{div}(\alpha_L \mathbf{v}) = \frac{1}{\rho_L}(m^+ + m^-) \tag{2}$$

with source terms, responsible for evaporation and condensation. These are evaluated using ZGB model [10]:

$$m^{+} = C_{prod}(1-\alpha_L)\rho_V\sqrt{\frac{2}{3}\frac{\max[0,\, p-p_V]}{\rho_L}}, \qquad m^{-} = -C_{dest}\alpha_L\rho_V\sqrt{\frac{2}{3}\frac{\max[0,\, p_V-p]}{\rho_L}},$$

where $C_{prod} = 3\cdot10^4$, $C_{dest} = 7.5\cdot10^4$. Turbulence is modelled using Kim-Chen *k*-ε model.

Total specific energy E_2 at draft tube outlet is obtained from a given Thoma number σ and net head H according to IEC 60193 standard

$$E_2 = \sigma H + \frac{p_V}{\rho_L g} - z_r\,, \tag{3}$$

where z_r is the reference level, evaluated from the upper ring of wicket gate ($z = 0$). This condition is accompanied by the hydrostatic equation $\partial p / \partial z = \rho_L g$ in the draft tube outlet section. Total specific energy is also fixed at the inlet of the penstock

$$E_1 \equiv \left(h + \frac{Q^2}{2gA_1^2} \right) = E_2 + H = const\,.$$

Eq. (1) for penstock domain and RANS equations for turbine domain are solved simultaneously. Coupling of penstock and turbine flow parameters (discharge and pressure) is done by inner iterations at each time step. Numerical method is described in [8, 9, 11].

The above 1D-3D model accounts for the main factors responsible for excitation and evolution of full-load oscillations. These are flow inertia and compressibility of water in the penstock, cavitation development in draft tube cone and between runner blades (essential for low Thoma numbers). The main advantage of the model against fully 1D ones is a proper 3D link of cavity volume V_c to discharge and pressure variations.

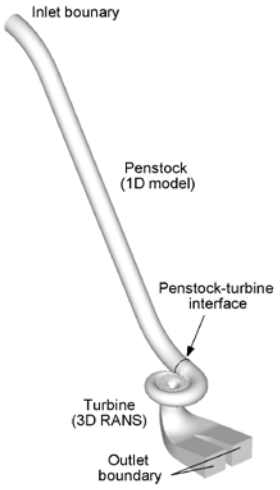

Fig.1 The concept of 1D-3D model.

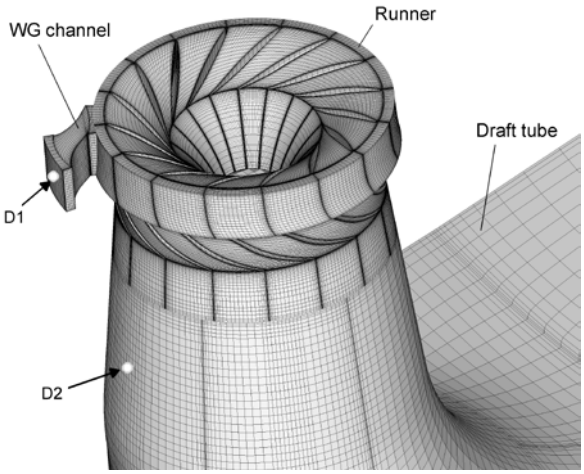

Fig.2 Mesh for "periodic WG – whole runner –draft tube" computations and monitoring points D1 (WG) and D2 (DT).

3. FULL RUNNER COMPUTATIONS

3D unsteady computations in the whole flow passage of Francis turbine are time consuming. Fortunately, for the case of full load surge computational domain can be significantly reduced. First, as it was suggested in [8], spiral casing and stay vanes can be excluded and represented by their pressure drop. Next, wicket gate (WG) can be computed within periodic approach, requiring computations in only one WG channel. In [9] the same approach was used also for the runner with circumferential averaging of all flow parameters on mixing plane between runner and draft tube (DT). This simplification is quite affordable for modern turbines, where the flow behind the runner is nearly axially symmetric in full and over-load

operating points. However, this is not true for some runner designs. Old runner R1, considered in [9] is the case. Due to the lack of axial velocity near the hub, swirling flow in the upper part of the draft tube cone becomes asymmetric, pointing out that periodic mixing plane approach may be not adequate for this case.

In the present paper, whole runner computations are carried out for R1 runner to ensure proper interaction of runner and draft tube. Fig. 2 shows computational mesh for R1 runner, consisting of one WG channel, all runner channels and the whole draft tube. No averaging is applied in runner-DT interface. Time step is 1/96 of runner rotation period, which is 4 times smaller than in periodic runner computations, performed in [9]. Fig. 3 compares pressure pulsations monitored in WG entrance (point D1 in Fig. 2) for two computations. Fig. 4 shows evolution of asymmetric vapor cavity within one pulsation period, obtained in whole runner simulation. Though in whole runner approach pressure pulsations seem to be more periodic, their frequency and average amplitude are approximately the same as in simple periodic computation. This fact, established for old-fashion runner, confirms the applicability of periodic runner approach for simulation of full load surge.

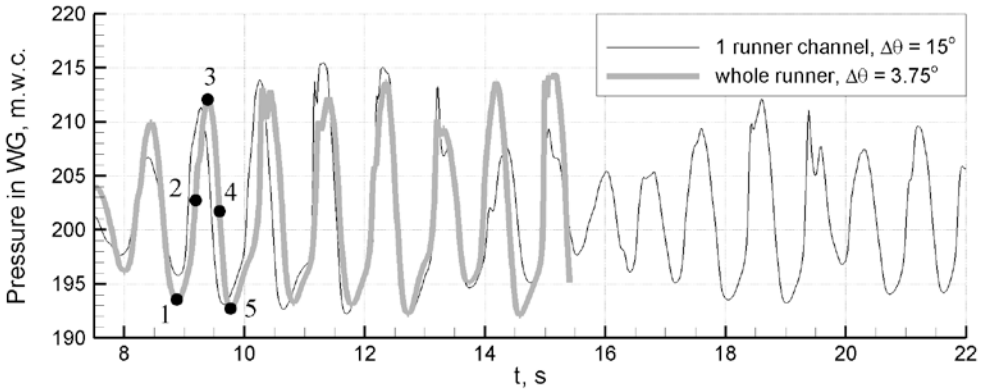

Fig. 3. Comparison of periodic and full runner computations for R1: pressure in WG.

1 2 3 4 5

Fig. 4. Vapor cavity in runner and draft tube for 5 moments of 1 period, see Fig.3.

4. INFLUENCE OF THOMA NUMBER

Fig. 5 shows the influence of Thoma number σ on pressure pulsations in WG for R2 turbine, operated at 110% of rated power. Periodic stage approach is used with time step $\Delta t = T_n / 24$. It can be seen that pulsations with highest amplitude, observed at $\sigma = 0.06$ and $\sigma = 0.08$, are the most periodic. Average frequencies (line "1") and amplitudes of pressure pulsations in WG (point D1) and DT (point D2, see Fig. 2) as functions of Thoma number are shown in Fig. 6. Almost linear increase of frequency with Thoma number, seen in Fig. 6, coincides with experimental observations of A. Muller [5]. However, in contrary to [5], the change of amplitude is not monotonic. Fig. 7, 8 show vapor cavity on runner blades and in DT in 7 time moments within 1 period of pulsations, for $\sigma = 0.06$ and $\sigma = 0.08$. The formation of helical vortex rope behind the main cavity can be observed for $\sigma = 0.08$.

One of the problems in investigation of full-load self-oscillations is the comparison of fully 1D hydro-acoustic models to 3D CFD computations. Fig. 9 shows the dependency of

first unstable frequency on cavitation compliance *C*, found from eigenvalue analysis of 1D model, described in [9]. Frequency, evaluated using simple formula $f = 1/2\pi\sqrt{C \cdot I_2}$ is also shown. Here $I_2 = L_2 / gA_2$ is the inertia of draft tube flow; L_2 and A_2 are the length and equivalent cross section area of the DT, respectively. Good agreement can be seen in practical range ($C > 0.1\,\mathrm{m}^2$). The problem is now to find *C*. In [9] we considered the case $\sigma = 0.08$ and identified $C = 0.135$ from 2 steady state two-phase computations with 2 different pressure levels in the outlet section. The resulting 1D frequency $f / f_n = 0.59$ fell far from 1D-3D result $f / f_n = 0.356$ [9].

Here we identified the value of *C* from the results of unsteady 1D-3D computations. For that, following [12], we plotted cavity volume V_c against pressure in DT, monitored in point D2. Fig. 10 shows the obtained V_c loops for several values of Thoma number. For $\sigma = 0.06$ the volume of vapor phase in the runner was also included in V_c. In order to get a single value of cavitation compliance $C = -\partial V_c / \partial p[m.w.c]$, linear approximation of $V_c(p)$ curve was constructed for each σ, see Fig. 10. The resulting frequencies, see Fig. 9, are shown also in Fig. 6 (line "2"). Good agreement with 1D-3D results can be seen now.

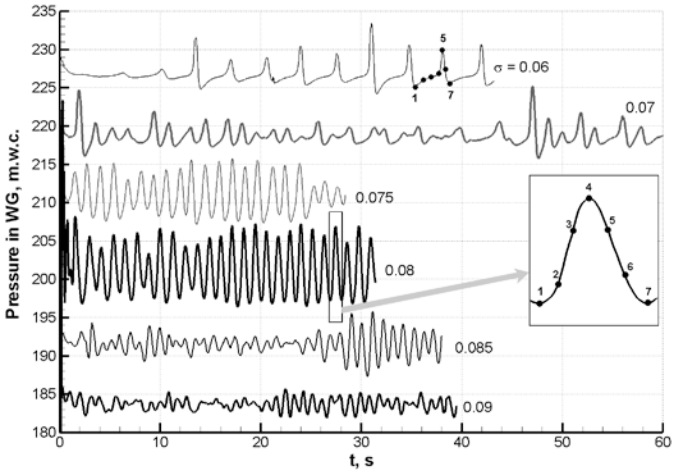

Fig. 5. Pressure pulsations in WG for various σ. Note, pressure levels are shifted for the sake of visualization.

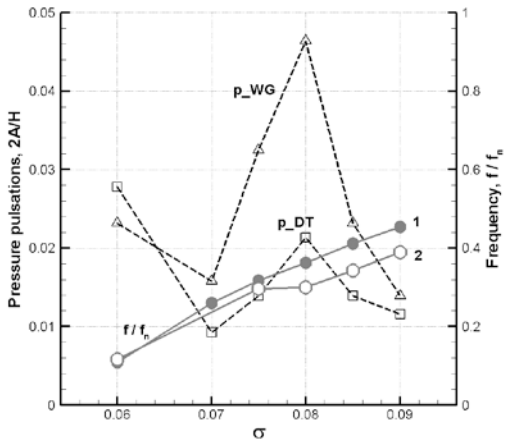

Fig. 6. Amplitude and frequency and of pressure pulsations versus σ.

Fig. 7. Evolution of vapor cavity in runner and draft tube, $\sigma = 0.06$.

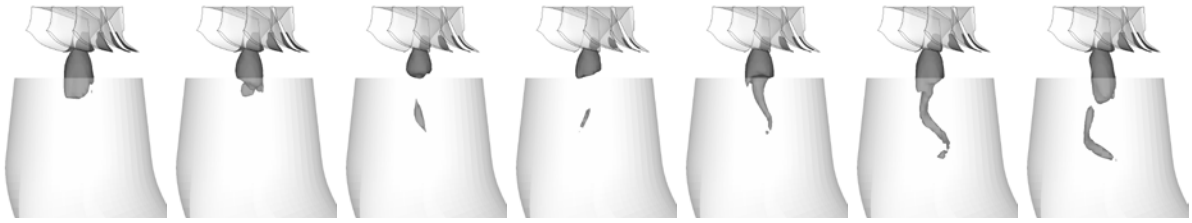

Fig. 8. Evolution of vapor cavity in runner and draft tube, $\sigma = 0.08$.

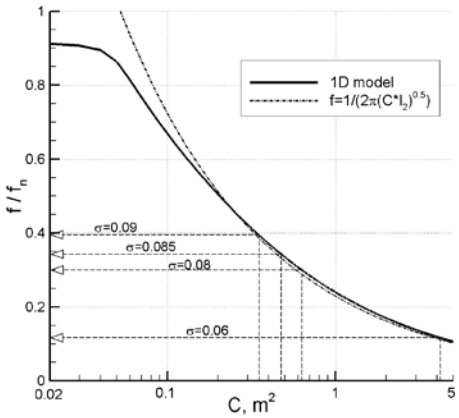

Fig. 9. First unstable frequency as function of cavitation compliance.

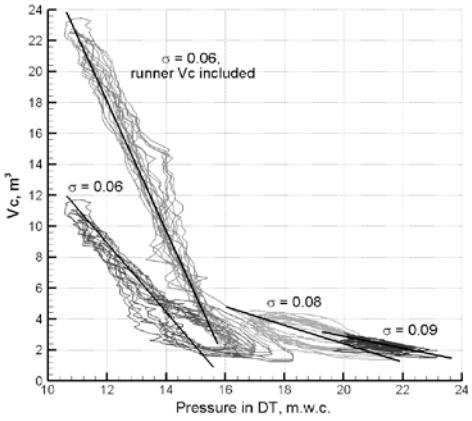

Fig. 10. Identification of cavitation compliance: cavity volume Vc against pressure in DT.

5. INFLUENCE OF DISCHARGE

The main interest is the dependence of pressure and power pulsation amplitudes on average turbine power, since it determines the upper limit of stable operation. In order to evaluate these dependencies 5 unsteady computations for various guide vane openings at constant net head have been carried out, corresponding to 110%, 115%, 117.5%, 119% and 123% of rated output power P_{rated}. As in Sec. 4, turbine with new R2 runner is considered. Fig. 11 shows the resulting pressure fluctuations in wicket gate. It can be seen, that at 110% of rated power the pulsations are almost negligible. The increase of power leads to drastic growth of pressure pulsation amplitudes, both in WG and DT (see also Fig. 12). At 117.5% of P_{rated} peak-to-peak amplitude of pressure pulsations in WG reaches 4.6% of the net head. Further increase of load reduces the amplitude of pulsations. It can be seen that for all regimes with pronounced oscillations, the amplitudes in WG are about 2 times higher than those in the draft tube. Frequency monotonically decreases as discharge grows, from 0.6 to 0.2 of runner rotation frequency. This behaviour is again in qualitative agreement with model experiments [5]. Line "2" in Fig. 12 shows the frequency, obtained in frames of fully 1D model with cavitation compliance *C*, identified from unsteady 1D-3D simulations, as described in Sec. 4. Again, the 1D frequency is close to 1D-3D result.

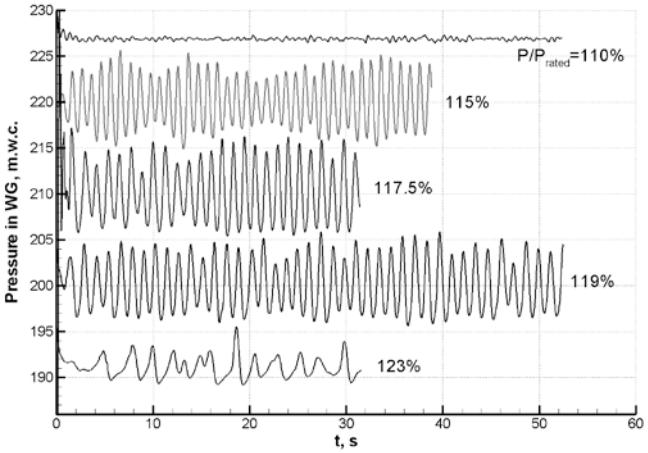

Fig. 11. Pressure pulsations in WG for various output power.

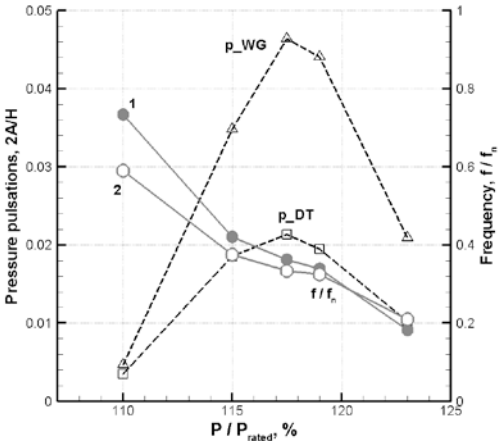

Fig. 12. Amplitude and frequency of pressure pulsations versus output power.

Synchronous pressure pulsations result in severe power oscillations of the same frequency. Fig. 13 compares peak-to-peak power oscillations, measured in prototype turbine (with R1 runner) with those, obtained in present 1D-3D simulations for R1 and R2 runners.

Abrupt increase of power pulsations beyond about 107% of rated power is well predicted. It can also be seen that the onset of instability for the new R2 runner is shifted to the right to about 3% of P_{rated} and the amplitude of power pulsations are 2 times smaller than for old R1 runner.

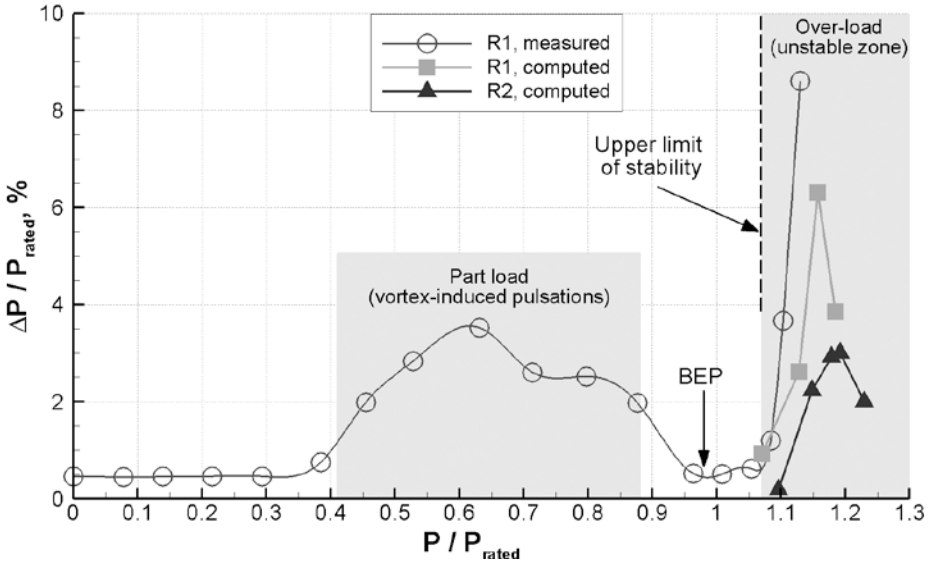

Fig. 13. Peak-to-peak amplitude of power pulsations as function of average turbine power.

6. CONCLUSION

Recently developed 1D-3D model of hydro-acoustic pulsations in power plant is further investigated and applied to the prediction of limit of stable operation at high discharge. Series of computations with various guide vane openings and Thoma numbers have been carried out for prototype turbine. The obtained results indicate strong influence of these parameters on frequency and amplitude of full load pulsations. Evaluated dependencies outline the zone of operating points with high amplitude of pressure and power pulsations and thus provide the upper limit of stable operation at high load. The computed amplitudes of power pulsations are in good agreement with experimental data measured in prototype, showing applicability of the model to predict full load pulsations.

The frequencies of computed pressure pulsations are compared with first unstable frequencies, obtained in fully 1D model. It is shown that if cavitation compliance, used as the input in 1D model, is taken from unsteady 1D-3D computations, then 1D and 1D-3D frequencies are close to each other. This fact establishes the bridge between 3D CFD and fully 1D models of full load surge.

It is shown that onset and the amplitude of self-oscillations strongly depend on runner geometry. This fact indicates the possibility to reduce or even eliminate high-load pulsations with proper runner design.

The next challenge is to introduce third phase (non-condensable air) into the model in order to investigate the effect of air admission behind the runner.

7. ACKNOWLEDGEMENTS

This work was supported by grant № 14-01-00278 of Russian Foundation for Basic Research.

8. REFERENCES

[1] Jacob T. and Prenat J.-E.: Francis Turbine Surge: Discussion and Data Base. *IAHR Symp. on Hydraulic Machinery and Systems* (Valencia, Spain). 1996.

[2] Dörfler P., Sick M., Coutu A.: *Flow-Induced Pulsation and Vibration in Hydroelectric Machinery*. Springer-Verlag, London. 2013. 242 p.

[3] Koutnik J., Nicolet C., Schohl G. A., and Avellan F.: Overload surge event in a pumped storage power plant. *IAHR Symp. on Hydraulic Machinery and Systems* (Yokohama, Japan). 2006.

[4] Alligne S., Maruzewski P., Dinh T., Wang B., Fedorov A., Iosfin J. and Avellan F.: Prediction of a Francis turbine prototype full load instability from investigations on the reduced scale model. *IAHR Symp. on Hydraulic Machinery and Systems* (Timisoara, Romania). 2010.

[5] Muller A.: Physical Mechanisms governing self-excited pressure oscillations in Francis turbines. Ph. D. Thesis EPFL No. 6206. 2014.

[6] Nicolet C.: Hydroacoustic modelling and numerical simulation of unsteady operation of hydroelectric systems. Ph. D. Thesis EPFL No. 3751. 2007.

[7] Chen C., Nicolet C., Yonezawa K., Farhat M., Avellan F., Tsujimoto Y.: One-dimensional analysis of full load draft tube surge. *J. of Fluids Engineering.* Vol. 130. 2008.

[8] Chirkov D., Avdyushenko A., Panov L., Bannikov D., Cherny S., Skorospelov V., Pylev I.: CFD simulation of pressure and discharge surge in Francis turbine at off-design conditions. *IAHR Symp. on Hydraulic Machinery and Systems* (Beijing, China). 2012.

[9] Chirkov D., Panov L., Cherny S., Pylev I.: Numerical simulation of full load surge in Francis turbines based on three-dimensional cavitating flow model // *IAHR Symp. on Hydraulic Machinery and Systems* (Montreal, Canada). 2014.

[10] Zwart P. J., Gerber A. G., Belamri T. A.: Two-phase flow model for predicting cavitation dynamics. *International Conference on Multiphase Flow* (Yokohama, Japan). Paper No. 152. 2004.

[11] Panov L.V., Chirkov D. V., Cherny S. G., Pylev I. M. and Sotnikov A. A.: Numerical modeling of steady-state cavitational flow of viscous fluid in Francis hydroturbine. *Thermophysics and Aeromechanics.* 2012. Vol. 19, No. 3. pp. 415-427.

[12] Chen C., Nicolet C., Yonezawa K., Farhat M., Avellan F., Miyagawa K., Tsujimoto Y. Experimental study and numerical simulation of cavity oscillation in a conical diffuser *Int. J. of Fluid Machinery and Systems.* 2010 Vol. 3**,** No. 1, pp. 91-101.

9. NOMENCLATURE

a	(m/s)	wave speed	H	(m)	net head
A	(m^2)	cross section area	n_q	(-)	specific speed
α_L	(-)	liquid volume fraction	p	(Pa)	pressure
C	(m^2)	cavity compliance	p_V	(Pa)	vapor pressure
χ	(s)	mass flow gain factor	P	(MW)	power
E	(m)	total specific energy	ρ_L	(kg/m^3)	water density
f	(Hz)	frequency	ρ_V	(kg/m^3)	vapor density
f_n	(Hz)	runner frequency	σ	(-)	Thoma number
g	(m/s2)	gravity acceleration	V_c	(m^3)	cavity volume
h	(m)	piezometric head			